

海洋地震工程流固耦合问题统一计算框架¹⁾

陈少林²⁾ 柯小飞 张洪翔

(南京航空航天大学土木工程系, 南京 210000)

摘要 海底地震动的模拟以及海洋工程结构的地震反应分析中, 涉及到海水、饱和海床、弹性基岩、结构之间的相互耦合. 传统的方法分别采用声波方程描述理想流体、Biot 方程描述饱和海床、弹性波方程描述基岩和结构, 分别考虑相互之间的耦合, 十分不便. 本文基于理想流体、固体分别为饱和多孔介质的特殊情形(孔隙率分别为 1 和 0), 由饱和多孔介质的 Biot 方程可退化得到理想流体的声波方程和固体的弹性波方程. 然后, 以饱和多孔介质方程为基础, 经集中质量有限元离散, 考虑不同孔隙率的饱和多孔介质之间耦合的一般情形, 建立了该耦合情形的求解方法. 进一步论证了该一般情形的耦合计算方法可分别退化到流体与固体、流体与饱和多孔介质、固体与饱和多孔介质之间的耦合计算, 从而将流体、固体、饱和多孔介质间的耦合问题纳入到统一计算框架, 并编制了相应的三维并行分析程序. 以 P-SV 波垂直入射时, 半无限层状海水-饱和海床、海水-弹性基岩、海水-饱和海床-弹性基岩三种情形的动力分析为例, 采用统一计算框架结合透射边界条件进行求解, 并与传递矩阵方法得到的解进行对比, 验证了该统一计算框架的有效性以及并行计算的可行性.

关键词 流固耦合, 饱和多孔介质, 海洋地震工程, 集中质量显式有限元, 透射边界, 并行计算

中图分类号: TU435 文献标识码: A doi: 10.6052/0459-1879-18-333

A UNIFIED COMPUTATIONAL FRAMEWORK FOR FLUID-SOLID COUPLING IN MARINE EARTHQUAKE ENGINEERING¹⁾

Chen Shaolin²⁾ Ke Xiaofei Zhang Hongxiang

(Department of Civil Engineering, Nanjing University of Aeronautics and Astronautics, Nanjing 210016, China)

Abstract The simulation of seismic wavefield at seafloor and seismic response of marine structures involves the coupling between seawater, saturated seabed, elastic bedrock and structure. That means, we target simulation where several types of equations are involved such as fluid, solid and saturated porous media equation. The conventional method for this fluid-solid-saturated porous media interaction problem is to use existing solvers of different equations and coupling method, which needs data mapping, communication and coupling algorithm between different solvers. Here, we present an alternative method, in which the coupling between different solvers is avoided. In fact, when porosity equals to one and zero, the saturated porous media is reduced to fluid and solid respectively, so we can use the porous media equation to describe the ideal fluid and solid, and the coupling between porous media, solid and fluid turns to the coupling between porous media with different porosity. Based on this idea, firstly the Biot's equations are approximated by Galerkin scheme and the explicit lumped-mass FEM is chosen, that are well suited to parallel computation. Then considering the traction

2018-10-12 收稿, 2018-12-18 录用, 2018-12-18 网络版发表.

1) 国家自然科学基金资助项目 (51178222, 51278260).

2) 陈少林, 教授, 主要研究方向: 地震工程. E-mail: icmcs1@nuaa.edu.cn

引用格式: 陈少林, 柯小飞, 张洪翔. 海洋地震工程流固耦合问题统一计算框架. 力学学报, 2019, 51(2): 594-606

Chen Shaolin, Ke Xiaofei, Zhang Hongxiang. A unified computational framework for fluid-solid coupling in marine earthquake engineering. *Chinese Journal of Theoretical and Applied Mechanics*, 2019, 51(2): 594-606

and velocity continuity on the interface between porous media with different porosity, the coupled algorithm is derived, which is proved to be suitable for the coupling between fluid, solid and saturated porous media. Thus, the coupling problem between fluid, solid and saturated porous media can be brought into a unified framework, in which only the solver of saturated porous media is used. The three-dimensional parallel code for this proposed method is programed, examples for analysis of layered water-saturated seabed, water-bedrock, and water-saturated seabed-bedrock semi-infinite systems subjected to plane P-SV wave are given, and the proposed unified framework is verified through comparison between the results obtained through the proposed unified framework combined with transmitting boundary condition and those obtained through transfer matrix method.

Key words fluid-solid coupling, saturated porous medium, marine earthquake engineering, explicit lumped-mass finite element method, transmitting boundary, parallel computation

引言

在海洋地震工程领域，需要关注海底地震波的传播^[1-2]及海底地震作用下结构的安全性问题^[3-6]，其响应分析涉及流固耦合问题。总体上，流固耦合从机理上可分为两类：一类是耦合作用仅仅发生在流体和固体介质的交界面上，由界面协调条件引入的^[7-16]；另一类是流固两相混合在一起，难以明显分开，其耦合效应通过描述问题的微分方程来体现，如描述饱和和多孔介质的 Biot 方程^[17-18]。在海洋工程中，海床土一般为饱和土，通过 Biot 方程进行描述，属于第二类流固耦合，海水与饱和海床之间的耦合、海水与结构(或基岩)间的耦合、以及饱和海床土与基岩(或结构)之间的耦合属于第一类流固耦合。因此，海洋工程中的流固耦合问题十分复杂，计算较为困难。若采用现行方法，需不同分析模块之间进行交互耦合^[19]。

地震波作用下，海水的响应一般通过声波方程进行描述。Komatitsch 等^[20]考虑海水与基岩界面法向速度连续和应力连续，建立平衡方程的耦合弱积分形式，通过谱元离散和显式 Newmark 时间积分，得到海底地震波的谱元模拟方法。李伟华等^[21]考虑理想流体和饱和土层的界面连续条件，建立了水与饱和场地耦合的显式有限元动力分析方法。两种方法均对海水、基岩和饱和土采用不同方程，分别离散，再通过界面条件进行耦合求解，十分不便。

理论上，固体和流体介质均为饱和和多孔介质的特殊情形，孔隙率分别为 0 和 1，上述耦合均可在饱和和多孔介质理论体系进行描述，如图 1 所示。基于此，本文从饱和和多孔介质的一般情形出发，考虑不同孔隙率的饱和和多孔介质之间的耦合，从而将上述所有耦合统一在同一计算框架，避免不同模块之间

的交互。另外，采用集中质量显式有限元方法，避免求解大型线性方程组，效率较高，且易于实现并行计算，有望用于大型海底地震波的模拟以及大型海工结构的地震反应分析。对于上述问题，需要采用人工边界模拟无限域的影响，一般采用透射边界^[22-23]和黏弹性边界^[24-25]，并分别以自由场^[26]和等效力^[27]作为输入。

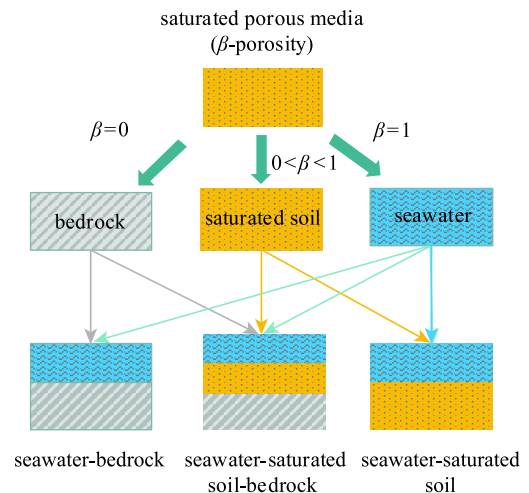


图 1 介质关系示意图

Fig. 1 Schematic diagram of media relations

1 基本理论

1.1 一般饱和和多孔介质情形

饱和和多孔介质的固相平衡方程

$$\mathbf{L}_s^T \boldsymbol{\sigma}' - (1 - \beta) \mathbf{L}_w^T P + b(\dot{\mathbf{U}} - \dot{\mathbf{u}}) = (1 - \beta) \rho_s \ddot{\mathbf{u}} \quad (1)$$

液相平衡方程

$$-\beta \mathbf{L}_w^T P + b(\dot{\mathbf{u}} - \dot{\mathbf{U}}) = \beta \rho_w \ddot{\mathbf{U}} \quad (2)$$

相容方程 (考虑初始孔压和初始体应变为零时)

$$\tau = -\beta P = E_w[\beta e^w + (1 - \beta)e^s] \quad (3)$$

其中, \mathbf{L}_s 和 \mathbf{L}_w 为微分算子矩阵; $\boldsymbol{\sigma}'$ 为有效应力矢量, τ 为平均孔压, 以拉为正; P 为孔隙水压, 以压为正; \mathbf{U} 和 \mathbf{u} 分别为液相和固相的位移矢量, $\dot{\mathbf{U}}$ 和 $\dot{\mathbf{u}}$ 为速度, $\ddot{\mathbf{U}}$ 和 $\ddot{\mathbf{u}}$ 为加速度; ρ_s 和 ρ_w 分别为固相和液相的密度, β 为孔隙率, $b = \beta^2 \mu_0 / k_0$, k_0 为流体渗透系数, μ_0 为动黏度系数; E_w 为流体的体变模量, e^s 和 e^w 分别为固相和液相的体应变, \mathbf{e} 为固相的应变矢量. \mathbf{L}_s 和 \mathbf{L}_w 分别为

$$\mathbf{L}_s = \begin{bmatrix} \partial/\partial x_1 & 0 & 0 \\ 0 & \partial/\partial x_2 & 0 \\ 0 & 0 & \partial/\partial x_3 \\ \partial/\partial x_2 & \partial/\partial x_1 & 0 \\ 0 & \partial/\partial x_3 & \partial/\partial x_2 \\ \partial/\partial x_3 & 0 & \partial/\partial x_1 \end{bmatrix} \quad (4a)$$

$$\mathbf{L}_w = (\partial/\partial x_1, \partial/\partial x_2, \partial/\partial x_3) \quad (4b)$$

Dirichlet 边界条件

$$\mathbf{u} - \bar{\mathbf{u}} = \mathbf{0} \quad (5a)$$

$$\mathbf{U} - \bar{\mathbf{U}} = \mathbf{0} \quad (5b)$$

Neumann 边界条件

$$\hat{\mathbf{n}}\boldsymbol{\sigma} - \bar{\boldsymbol{\sigma}} = \mathbf{0} \quad (5c)$$

$$(P - \bar{P})\mathbf{n} = \mathbf{0} \quad (5d)$$

其中, $\bar{\mathbf{u}}$ 和 $\bar{\mathbf{U}}$ 分别为在边界上给定的固相和液相位移. $\bar{\boldsymbol{\sigma}}$ 和 \bar{P} 分别为边界上固相平均应力和真实孔压的给定值; \mathbf{n} 为沿边界外法线的方向矢量, $\hat{\mathbf{n}}$ 为由方向导数组成的矩阵, 其形式如下

$$\mathbf{n} = (n_x, n_y, n_z)^T \quad (6a)$$

$$\hat{\mathbf{n}} = \begin{bmatrix} n_x & 0 & 0 & n_y & 0 & n_z \\ 0 & n_y & 0 & n_x & n_z & 0 \\ 0 & 0 & n_z & 0 & n_y & n_x \end{bmatrix} \quad (6b)$$

对方程 (1) 和 (2) 采用伽辽金方法离散, 考虑边界条件, 可得任一结点 i 的解耦运动平衡方程为 [28]

$$\ddot{\mathbf{u}}_i \mathbf{M}_{si} + \mathbf{F}_i^s + \mathbf{T}_i^s - \mathbf{S}_i^s = \mathbf{0} \quad (7)$$

$$\ddot{\mathbf{U}}_i \mathbf{M}_{wi} + \mathbf{F}_i^w + \mathbf{T}_i^w - \mathbf{S}_i^w = \mathbf{0} \quad (8)$$

其中, \mathbf{M}_{si} 和 \mathbf{M}_{wi} 分别为集中在 i 节点上的固相质量和液相质量; \mathbf{F}_i^s 和 \mathbf{F}_i^w 分别为集中在节点 i 的固、液相本构力; \mathbf{T}_i^s 和 \mathbf{T}_i^w 分别为集中在节点 i 的固、液相黏性阻力; \mathbf{S}_i^s 和 \mathbf{S}_i^w 分别作用在节点 i 的固、液相边界力. 在同一介质内, 由于所有位移和应力都连续, 通过单元界面作用在它们之上的应力大小相等、方向相反, 在单元组装的过程中, 内部节点的 \mathbf{S}_i^s 和 \mathbf{S}_i^w 均为零. 它们由下面的式子计算得到

$$\mathbf{M}_{si} = \sum_e \sum_{j=1}^J \int_{\Omega^e} \mathbf{N}_i^T (1 - \beta) \rho_s \mathbf{N}_j dV \quad (9a)$$

$$\mathbf{M}_{wi} = \sum_e \sum_{j=1}^J \int_{\Omega^e} \mathbf{N}_i^T \beta \rho_w \mathbf{N}_j dV \quad (9b)$$

$$\mathbf{T}_i^s = \sum_e \int_{var\Omega^e} \mathbf{N}_i^T b \mathbf{N}_j (\dot{\mathbf{u}}_j - \dot{\mathbf{U}}_j) dV \quad (9c)$$

$$\mathbf{T}_i^s = \sum_e \int_{\Omega^e} \mathbf{N}_i^T b \mathbf{N}_j (\dot{\mathbf{u}}_j - \dot{\mathbf{U}}_j) dV \quad (9d)$$

$$\mathbf{T}_i^s = \sum_e \int_{\Omega^e} \mathbf{N}_i^T b \mathbf{N}_j (\dot{\mathbf{u}}_j - \dot{\mathbf{U}}_j) dV \quad (9e)$$

$$\mathbf{S}_i^s = \sum_e \int_{S^e} \mathbf{N}_i^T \hat{\mathbf{n}} \boldsymbol{\sigma} dS \quad (9f)$$

$$\mathbf{S}_i^s = \sum_e \int_{S^e} \mathbf{N}_i^T \hat{\mathbf{n}} \boldsymbol{\sigma} dS \quad (9g)$$

$$\mathbf{S}_i^w = \sum_e \int_{S^e} \mathbf{N}_i^T \mathbf{n} \beta P dS \quad (9h)$$

若节点 i 为内部节点 (非界面点), \mathbf{S}_i^s 和 \mathbf{S}_i^w 均为零, 给定本构关系, 可对式 (7)、式 (8) 式采用时步积分求解 [28]. 这里讨论节点 i 为两种不同介质的界面点情形, 如图 2 所示. 采用隔离体概念, 则介质一中界面点 i 的动力方程由式 (7)、式 (8) 描述, 介质二中界面点 k 的动力方程表示如下 (除微分算子和形函

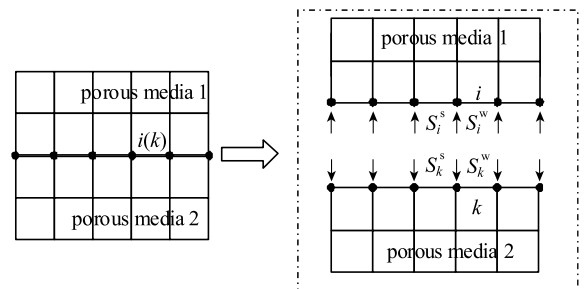


图 2 界面受力示意图

Fig. 2 Schematic diagram of interfacial force

数外，其他物理量均带上划线，以区别于介质一)

$$\bar{\mathbf{u}}_k \bar{\mathbf{M}}_{sk} + \bar{\mathbf{F}}_k^s + \bar{\mathbf{T}}_k^s - \bar{\mathbf{S}}_k^s = \mathbf{0} \quad (10)$$

$$\bar{\mathbf{U}}_k \bar{\mathbf{M}}_{wk} + \bar{\mathbf{F}}_k^w + \bar{\mathbf{T}}_k^w - \bar{\mathbf{S}}_k^w = \mathbf{0} \quad (11)$$

其中

$$\bar{\mathbf{M}}_{sk} = \sum_e \sum_{j=1}^J \int_{\Omega^e} N_k^T (1 - \bar{\beta}) \bar{\rho}_s N_j dV \quad (12a)$$

$$\bar{\mathbf{M}}_{wk} = \sum_e \sum_{j=1}^J \int_{\Omega^e} N_k^T \bar{\beta} \bar{\rho}_w N_j dV \quad (12b)$$

$$\bar{\mathbf{F}}_k^s = \sum_e \bar{\mathbf{f}}_k^{se} = \sum_e \int_{\Omega^e} (\mathbf{L}_s N_k)^T \bar{\boldsymbol{\sigma}} dV \quad (12c)$$

$$\bar{\mathbf{F}}_k^w = \sum_e \bar{\mathbf{f}}_k^{we} = \sum_e \int_{\Omega^e} (\mathbf{L}_w N_k)^T \bar{\beta} \bar{\mathbf{P}} dV \quad (12d)$$

$$\bar{\mathbf{T}}_k^s = \sum_e \int_{\Omega^e} N_k^T \bar{\mathbf{b}} N_j (\dot{\mathbf{u}}_j - \dot{\mathbf{U}}_j) dV \quad (12e)$$

$$\bar{\mathbf{T}}_k^w = -\bar{\mathbf{T}}_k^s \quad (12f)$$

$$\bar{\mathbf{S}}_k^s = \sum_e \int_{S^e} N_k^T \bar{\mathbf{n}} \bar{\boldsymbol{\sigma}} dS \quad (12g)$$

$$\bar{\mathbf{S}}_k^w = \sum_e \int_{S^e} N_k^T \bar{\mathbf{n}} \bar{\beta} \bar{\mathbf{P}} dS \quad (12h)$$

此时， \mathbf{S}_i^s 和 \mathbf{S}_i^w 为介质二作用在界面点 i 上的界面力， $\bar{\mathbf{S}}_k^s$ 和 $\bar{\mathbf{S}}_k^w$ 为介质一作用在界面点 k 上的界面力，它们之间的关系由如下界面连续条件^[30]确定

$$\sigma_{zz} + \tau = \bar{\sigma}_{zz} + \bar{\tau} \quad (13a)$$

$$\sigma_{zx} = \bar{\sigma}_{zx}, \sigma_{zy} = \bar{\sigma}_{zy} \quad (13b)$$

$$P - \bar{P} = k' \beta (\dot{U}_z - \dot{u}_z) \quad (13c)$$

$$\dot{u}_x = \bar{\dot{u}}_x, \dot{u}_y = \bar{\dot{u}}_y \quad (13d)$$

$$\dot{u}_z = \bar{\dot{u}}_z, \beta (\dot{U}_z - \dot{u}_z) = \bar{\beta} (\bar{\dot{U}}_z - \bar{\dot{u}}_z) \quad (13e)$$

其中，式 (13c) 中的 k' 为阻滞系数，这里假设两种介质的孔隙完全连通， $k' = 0$ 。另外，假设系统的初始值为零，则式 (13d)、式 (13e) 中的速度可换成位移和加速度，本文的推导中采用这一假设。将式 (7) 和式 (10) 中 x 方向的方程相加，考虑到式 (13d) 和式 (13b)，以及 $\hat{\mathbf{n}} = -\bar{\hat{\mathbf{n}}}$ ，有

$$\bar{\mathbf{u}}_{kx} (m_{si} + \bar{m}_{sk}) + F_{ix}^s + \bar{F}_{kx}^s + T_{ix}^s + \bar{T}_{kx}^s = 0 \quad (14)$$

这即是通常的单元组装后，节点 k 的 x 方向平衡方程。同理，可得节点 k 的 y 方向固相方程如下

$$\bar{\mathbf{u}}_{ky} (m_{si} + \bar{m}_{sk}) + F_{iy}^s + \bar{F}_{ky}^s + T_{iy}^s + \bar{T}_{ky}^s = 0 \quad (15)$$

这里以水平成层介质为例，则方向导数 $n_x = n_y = -\bar{n}_x = -\bar{n}_y = 0$ ， $n_z = -\bar{n}_z = 1$ ，由式 (9h)、式 (12h) 可知， $S_{ix}^s = S_{iy}^s = 0$ ， $\bar{S}_{ix}^w = \bar{S}_{iy}^w = 0$ 。因此， i 点和 k 点在 x, y 方向的液相方程如下

$$m_{wi} \ddot{U}_{iy} + F_{iy}^w + T_{iy}^w = 0 \quad (16)$$

$$m_{wi} \ddot{U}_{iy} + F_{iy}^w + T_{iy}^w = 0 \quad (17)$$

$$\bar{m}_{wk} \ddot{U}_{kx} + \bar{F}_{kx}^w + \bar{T}_{kx}^w = 0 \quad (18)$$

$$\bar{m}_{wk} \ddot{U}_{ky} + \bar{F}_{ky}^w + \bar{T}_{ky}^w = 0 \quad (19)$$

取式 (7)、式 (8)、式 (10)、式 (11) 式的 z 方向方程相加，考虑到 $n_x = n_y = -\bar{n}_x = -\bar{n}_y = 0$ ， $n_z = -\bar{n}_z = 1$ ，由式 (13a) 可知， $S_{iz}^s + S_{iz}^w + \bar{S}_{kz}^s + \bar{S}_{kz}^w = 0$ ，故可得

$$\bar{m}_{sk} \bar{\mathbf{u}}_{kz} + \bar{m}_{wk} \bar{\mathbf{U}}_{kz} + m_{si} \ddot{u}_{iz} + m_{wi} \ddot{U}_{iz} + F_{iz}^s + F_{iz}^w + \bar{F}_{kz}^s + \bar{F}_{kz}^w + T_{iz}^s + T_{iz}^w + \bar{T}_{kz}^s + \bar{T}_{kz}^w = 0 \quad (20)$$

将式 (8) 乘以 $\bar{\beta}$ ，加上式 (11) 乘以 β ，取 z 方向的方程。由式 (9h)、式 (12h) 和式 (13c) 可知， $\bar{\beta} S_{iz}^w + \beta \bar{S}_{kz}^w = 0$ ，故可得

$$\bar{\beta} m_{wi} \ddot{U}_{iz} + \beta \bar{m}_{wk} \bar{\mathbf{U}}_{kz} + \bar{\beta} F_{iz}^w + \beta \bar{F}_{kz}^w + \bar{\beta} T_{iz}^w + \beta \bar{T}_{kz}^w = 0 \quad (21)$$

将式 (13e) 代入式 (20) 和式 (21)，消去 \ddot{u}_{iz} 、 \ddot{U}_{iz} ，整理得

$$A_{11} \bar{\mathbf{u}}_{kz} + A_{12} \bar{\mathbf{U}}_{kz} + B_{11} = 0 \quad (22)$$

$$A_{21} \bar{\mathbf{u}}_{kz} + A_{22} \bar{\mathbf{U}}_{kz} + B_{22} = 0 \quad (23)$$

其中

$$A_{11} = m_{si} + \bar{m}_{sk} + (1 - \bar{\beta}/\beta) m_{wi} \quad (24a)$$

$$A_{12} = \bar{m}_{wk} + (\bar{\beta}/\beta) m_{wi} \quad (24b)$$

$$A_{21} = \bar{\beta} (1 - \bar{\beta}/\beta) m_{wi} \quad (24c)$$

$$A_{22} = \beta \bar{m}_{wk} + (\bar{\beta}^2/\beta) m_{wi} + \varepsilon \quad (24d)$$

$$B_{11} = F_{iz}^s + F_{iz}^w + \bar{F}_{kz}^s + \bar{F}_{kz}^w + T_{iz}^s + T_{iz}^w + \bar{T}_{kz}^s + \bar{T}_{kz}^w \quad (24e)$$

$$B_{22} = \bar{\beta} F_{iz}^w + \beta \bar{F}_{kz}^w + \bar{\beta} T_{iz}^w + \beta \bar{T}_{kz}^w \quad (24f)$$

式 (24d) 中, 附加的 ε 为一非常小的量, 其作用是避免饱和多孔介质退化到流体和固体情形时, 分母为零. 联立式 (22)、式 (23), 可解得

$$\bar{u}_{kz} = \frac{A_{22}B_{11} - A_{12}B_{22}}{A_{21}A_{12} - A_{11}A_{22}} \quad (25)$$

$$\bar{U}_{kz} = \frac{A_{11}B_{22} - A_{21}B_{11}}{A_{21}A_{12} - A_{11}A_{22}} \quad (26)$$

式 (14)~ 式 (19), 以及式 (25) 和式 (26) 可采用时步积分求解. 本文采用如下显式积分格式

$$\dot{U}^p = \frac{1}{\Delta t^2}(U^{(p+1)} - 2U^p + U^{(p-1)}) \quad (27)$$

$$\dot{U}^p = \frac{1}{\Delta t}(U^p - U^{(p-1)}) \quad (28)$$

其中, 上标 p 表示 $t = p\Delta t$ 时刻. 对式 (14)~ 式 (19) 以及式 (25) 和式 (26) 式采用上述时步积分格式, 可得

$$\bar{u}_{kx}^{(p+1)} = 2\bar{u}_{kx}^p - \bar{u}_{kx}^{(p-1)} - \frac{\Delta t^2}{(m_{si} + \bar{m}_{sk})} (F_{ix}^{sp} + \bar{F}_{kx}^{sp} + T_{ix}^{sp} + \bar{T}_{kx}^{sp}) \quad (29a)$$

$$\bar{u}_{ky}^{(p+1)} = 2\bar{u}_{ky}^p - \bar{u}_{ky}^{(p-1)} - \frac{\Delta t^2}{(m_{si} + \bar{m}_{sk})} (F_{iy}^{sp} + \bar{F}_{ky}^{sp} + T_{iy}^{sp} + \bar{T}_{ky}^{sp}) \quad (29b)$$

$$\bar{u}_{kz}^{(p+1)} = 2\bar{u}_{kz}^p - \bar{u}_{kz}^{(p-1)} + \frac{A_{22}B_{11}^p - A_{12}B_{22}^p}{A_{21}A_{12} - A_{11}A_{22}} \Delta t^2 \quad (29c)$$

$$\bar{U}_{kx}^{(p+1)} = 2\bar{U}_{kx}^p - \bar{U}_{kx}^{(p-1)} - \frac{\Delta t^2}{\bar{m}_{wk}} (\bar{F}_{kx}^{wp} + \bar{T}_{kx}^{wp}) \quad (29d)$$

$$\bar{U}_{ky}^{(p+1)} = 2\bar{U}_{ky}^p - \bar{U}_{ky}^{(p-1)} - \frac{\Delta t^2}{\bar{m}_{wk}} (\bar{F}_{ky}^{wp} + \bar{T}_{ky}^{wp}) \quad (29e)$$

$$\bar{U}_{kz}^{(p+1)} = 2\bar{U}_{kz}^p - \bar{U}_{kz}^{(p-1)} + \frac{A_{11}B_{22}^p - A_{21}B_{11}^p}{A_{21}A_{12} - A_{11}A_{22}} \Delta t^2 \quad (29f)$$

$$U_{ix}^{(p+1)} = 2U_{ix}^p - U_{ix}^{(p-1)} - \frac{\Delta t^2}{m_{wi}} (F_{ix}^{wp} + T_{ix}^{wp}) \quad (29g)$$

$$U_{iy}^{(p+1)} = 2U_{iy}^p - U_{iy}^{(p-1)} - \frac{\Delta t^2}{m_{wi}} (F_{iy}^{wp} + T_{iy}^{wp}) \quad (29h)$$

得到 $\bar{u}_{kx}^{(p+1)}$, $\bar{u}_{ky}^{(p+1)}$, $\bar{u}_{kz}^{(p+1)}$, $\bar{U}_{kz}^{(p+1)}$ 后, 由式 (13d) 和式 (13e) 可进一步求得 $u_{ix}^{(p+1)}$, $u_{iy}^{(p+1)}$, $u_{iz}^{(p+1)}$, $U_{iz}^{(p+1)}$

$$u_{ix}^{(p+1)} = \bar{u}_{kx}^{(p+1)}, u_{iy}^{(p+1)} = \bar{u}_{ky}^{(p+1)}, u_{iz}^{(p+1)} = \bar{u}_{kz}^{(p+1)} \quad (29i)$$

$$U_{iz}^{(p+1)} = \bar{\beta}[\bar{\beta}(\bar{U}_{kz}^{(p+1)} - \bar{u}_{kz}^{(p+1)}) + \bar{u}_{kz}^{(p+1)}] \quad (29j)$$

因此, 由式 (29) 可得界面点 i 和 k 的响应.

1.2 特殊情形

1.2.1 流体-饱和土情形

考虑饱和土上覆流体情形. 此时, 图 2 中介质二为饱和多孔介质, 介质一为流体, $\beta = 1$, $\mathbf{M}_{si} = \mathbf{0}$. 考虑无黏的理想流体, 动黏度系数为零, 则 $b = 0$,

$\mathbf{T}_i^s = \mathbf{0}$, $\mathbf{T}_i^w = \mathbf{0}$; 不存在固相, 固相骨架模量可取为零, 则 $\mathbf{F}_i^s = \mathbf{0}$, $\mathbf{S}_i^s = \mathbf{0}$; 由此, 式 (7) 自动满足, 式 (8) 退化为如下理想流体方程

$$\dot{\mathbf{U}}_i \mathbf{M}_{wi} + \mathbf{F}_i^w - \mathbf{S}_i^w = \mathbf{0} \quad (30)$$

因此, 饱和多孔介质方程可以用来分析理想流体的动力响应.

流体-饱和土界面连续条件为 [28]

$$P = \bar{\sigma}_{zz} + \bar{\tau} \quad (31a)$$

$$P = \bar{P} \quad (31b)$$

$$\dot{U}_z = \bar{\beta}(\dot{\bar{U}}_z - \dot{\bar{u}}_z) + \dot{\bar{u}}_z \quad (31c)$$

由动力方程式 (10)、式 (11)、式 (30) 以及界面连续条件式 (31), 按 2.1 节的方法, 可得界面点的运动方程如下

$$\bar{u}_{kx}^{(p+1)} = 2\bar{u}_{kx}^p - \bar{u}_{kx}^{(p-1)} - \frac{\Delta t^2}{\bar{m}_{sk}} (\bar{F}_{kx}^{sp} + \bar{T}_{kx}^{sp}) \quad (32a)$$

$$\bar{u}_{ky}^{(p+1)} = 2\bar{u}_{ky}^p - \bar{u}_{ky}^{(p-1)} - \frac{\Delta t^2}{\bar{m}_{sk}} (\bar{F}_{ky}^{sp} + \bar{T}_{ky}^{sp}) \quad (32b)$$

$$\bar{u}_{kz}^{(p+1)} = 2\bar{u}_{kz}^p - \bar{u}_{kz}^{(p-1)} + \frac{A_{22}B_{11}^p - A_{12}B_{22}^p}{A_{21}A_{12} - A_{11}A_{22}} \Delta t^2 \quad (32c)$$

$$\bar{U}_{kx}^{(p+1)} = 2\bar{U}_{kx}^p - \bar{U}_{kx}^{(p-1)} - \frac{\Delta t^2}{\bar{m}_{wk}} (\bar{F}_{kx}^{wp} + \bar{T}_{kx}^{wp}) \quad (32d)$$

$$\bar{U}_{ky}^{(p+1)} = 2\bar{U}_{ky}^p - \bar{U}_{ky}^{(p-1)} - \frac{\Delta t^2}{\bar{m}_{wk}} (\bar{F}_{ky}^{wp} + \bar{T}_{ky}^{wp}) \quad (32e)$$

$$\bar{U}_{kz}^{(p+1)} = 2\bar{U}_{kz}^p - \bar{U}_{kz}^{(p-1)} + \frac{A_{11}B_{22}^p - A_{21}B_{11}^p}{A_{21}A_{12} - A_{11}A_{22}} \Delta t^2 \quad (32f)$$

$$U_{ix}^{(p+1)} = 2U_{ix}^p - U_{ix}^{(p-1)} - \frac{\Delta t^2}{m_{wi}} F_{ix}^{wp} \quad (32g)$$

$$U_{iy}^{(p+1)} = 2U_{iy}^p - U_{iy}^{(p-1)} - \frac{\Delta t^2}{m_{wi}} F_{iy}^{wp} \quad (32h)$$

$$U_{iz}^{(p+1)} = \bar{\beta}(\bar{U}_{kz}^{(p+1)} - \bar{u}_{kz}^{(p+1)}) + \bar{u}_{kz}^{(p+1)} \quad (32i)$$

其中

$$A_{11} = \bar{m}_{sk} + (1 - \bar{\beta})m_{wi} \quad (33a)$$

$$A_{12} = \bar{m}_{wk} + \bar{\beta}m_{wi} \quad (33b)$$

$$A_{21} = \bar{\beta}(1 - \bar{\beta})m_{wi} \quad (33c)$$

$$A_{22} = \bar{m}_{wk} + \bar{\beta}^2 m_{wi} \quad (33d)$$

$$B_{11}^p = F_{iz}^{wp} + \bar{F}_{kz}^{sp} + \bar{F}_{kz}^{wp} + \bar{T}_{kz}^{sp} + \bar{T}_{kz}^{wp} \quad (33e)$$

$$B_{22}^p = \bar{\beta}F_{iz}^{wp} + \bar{F}_{kz}^{wp} + \bar{T}_{kz}^{wp} \quad (33f)$$

将 $\beta = 1$, $\mathbf{M}_{si} = \mathbf{0}$, $\mathbf{F}_i^s = \mathbf{0}$, $\mathbf{T}_i^s = \mathbf{0}$, $\mathbf{T}_i^w = \mathbf{0}$, $\mathbf{F}_i^s = \mathbf{0}$, $\mathbf{S}_i^s = \mathbf{0}$ 代入式 (24) 和式 (29), 可分别得到式 (33) 和式 (32). 因此流体-饱和土耦合情形是两种不同多

孔介质耦合情形的特例, 可直接由 1.1 节中的理论进行分析.

1.2.2 饱和土-干基岩情形

图 2 中的介质二若为不透水的基岩, 不存在液相, 则 $\beta = 0$, $\bar{\mathbf{M}}_{\text{wk}} = \mathbf{0}$; 液相体积模量和固液之间的黏性力取为零, 则 $\bar{\mathbf{F}}_k^{\text{w}} = \mathbf{0}$, $\bar{\mathbf{T}}_k^{\text{w}} = \mathbf{0}$, $\bar{\mathbf{T}}_k^{\text{s}} = \mathbf{0}$, $\bar{\mathbf{S}}_k^{\text{w}} = \mathbf{0}$, 方程 (11) 自动满足, 式 (10) 退化为如下干基岩方程

$$\ddot{\mathbf{u}}_k \bar{\mathbf{M}}_{\text{sk}} + \bar{\mathbf{F}}_k^{\text{s}} - \bar{\mathbf{S}}_k^{\text{s}} = \mathbf{0} \quad (34)$$

因此, 饱和多孔介质方程可以用来分析干基岩的动力响应.

饱和土-干基岩界面条件为^[30]

$$\sigma_{zz} + \tau = \bar{\sigma}_{zz} \quad (35a)$$

$$\sigma_{zx} = \bar{\sigma}_{zx}, \sigma_{zy} = \bar{\sigma}_{zy} \quad (35b)$$

$$\dot{u}_x = \bar{u}_x, \dot{u}_y = \bar{u}_y \quad (35c)$$

$$\dot{u}_z = \bar{u}_z, \beta(\dot{U}_z - \dot{u}_z) = 0 \quad (35d)$$

由动力方程式 (7)、式 (8)、式 (34) 以及界面连续条件 (35) 式, 按 2.1 节的方法, 可得界面点的运动方程如下

$$\begin{aligned} \bar{u}_{kx}^{(p+1)} &= 2\bar{u}_{kx}^p - \bar{u}_{kx}^{(p-1)} - \Delta t^2 (F_{ix}^{\text{sp}} + \\ &\quad \bar{F}_{kx}^{\text{sp}} + T_{ix}^{\text{sp}}) / (m_{si} + \bar{m}_{sk}) \end{aligned} \quad (36a)$$

$$\begin{aligned} \bar{u}_{ky}^{(p+1)} &= 2\bar{u}_{ky}^p - \bar{u}_{ky}^{(p-1)} - \Delta t^2 (F_{iy}^{\text{sp}} + \\ &\quad \bar{F}_{ky}^{\text{sp}} + T_{iy}^{\text{sp}}) / (m_{si} + \bar{m}_{sk}) \end{aligned} \quad (36b)$$

$$\bar{u}_{kz}^{(p+1)} = 2\bar{u}_{kz}^p - \bar{u}_{kz}^{(p-1)} + B_{11}^p \Delta t^2 / A_{11} \quad (36c)$$

$$U_{ix}^{(p+1)} = 2U_{ix}^p - U_{ix}^{(p-1)} - \Delta t^2 (F_{ix}^{\text{wp}} + T_{ix}^{\text{wp}}) / m_{wi} \quad (36d)$$

$$U_{iy}^{(p+1)} = 2U_{iy}^p - U_{iy}^{(p-1)} - \Delta t^2 (F_{iy}^{\text{wp}} + T_{iy}^{\text{wp}}) / m_{wi} \quad (36e)$$

$$u_{ix}^{(p+1)} = \bar{u}_{ix}^{(p+1)} \quad (36f)$$

$$u_{iy}^{(p+1)} = \bar{u}_{iy}^{(p+1)} \quad (36g)$$

$$u_{iz}^{(p+1)} = \bar{u}_{iz}^{(p+1)} \quad (36h)$$

$$U_{iz}^{(p+1)} = \bar{u}_{iz}^{(p+1)} \quad (36i)$$

其中

$$A_{11} = m_{si} + \bar{m}_{sk} + m_{wi} \quad (37a)$$

$$B_{11}^p = F_{iz}^{\text{sp}} + F_{iz}^{\text{wp}} + \bar{F}_{kz}^{\text{sp}} + T_{iz}^{\text{sp}} + T_{iz}^{\text{wp}} \quad (37b)$$

将 $\beta = 0$, $\bar{\mathbf{M}}_{\text{wk}} = \mathbf{0}$, $\bar{\mathbf{F}}_k^{\text{w}} = \mathbf{0}$, $\bar{\mathbf{T}}_k^{\text{w}} = \mathbf{0}$, $\bar{\mathbf{T}}_k^{\text{s}} = \mathbf{0}$, $\bar{\mathbf{S}}_k^{\text{w}} = \mathbf{0}$ 代入式 (24) 和式 (29), 可分别得到式 (37) 和式 (36).

因此饱和土-干基岩耦合情形也是两种不同多孔介质耦合情形的特例, 可直接由 2.1 节中的理论进行分析.

1.2.3 流体-干基岩情形

此时, 图 2 中介质一为理想流体, 介质二为干基岩. 按前述参数取值, 运动方程分别退化式 (30) 和式 (34). 流体-干基岩界面连续条件为 (不透水)

$$P = \bar{\sigma}_{zz} \quad (38a)$$

$$\dot{U}_z = \bar{u}_z \quad (38b)$$

由动力方程 (30) 和 (34) 以及界面连续条件式 (38), 可得界面点的运动方程如下

$$\bar{u}_{kx}^{(p+1)} = 2\bar{u}_{kx}^p - \bar{u}_{kx}^{(p-1)} - \frac{\Delta t^2}{\bar{m}_{sk}} \bar{F}_{kx}^{\text{sp}} \quad (39a)$$

$$\bar{u}_{ky}^{(p+1)} = 2\bar{u}_{ky}^p - \bar{u}_{ky}^{(p-1)} - \frac{\Delta t^2}{\bar{m}_{sk}} \bar{F}_{ky}^{\text{sp}} \quad (39b)$$

$$\bar{u}_{kz}^{(p+1)} = 2\bar{u}_{kz}^p - \bar{u}_{kz}^{(p-1)} + \frac{B_{11}^p}{A_{11}} \Delta t^2 \quad (39c)$$

$$U_{ix}^{(p+1)} = 2U_{ix}^p - U_{ix}^{(p-1)} - \frac{\Delta t^2}{m_{wi}} F_{ix}^{\text{wp}} \quad (39d)$$

$$U_{iy}^{(p+1)} = 2U_{iy}^p - U_{iy}^{(p-1)} - \frac{\Delta t^2}{m_{wi}} F_{iy}^{\text{wp}} \quad (39e)$$

$$U_{iz}^{(p+1)} = \bar{u}_{iz}^{(p+1)} \quad (39f)$$

其中

$$A_{11} = \bar{m}_{sk} + m_{wi} \quad (40a)$$

$$B_{11}^p = F_{iz}^{\text{wp}} + \bar{F}_{kz}^{\text{sp}} \quad (40b)$$

同样, 将 $\beta = 1$, $\mathbf{M}_{si} = \mathbf{0}$, $\mathbf{F}_i^{\text{s}} = \mathbf{0}$, $\mathbf{T}_i^{\text{s}} = \mathbf{0}$, $\mathbf{T}_i^{\text{w}} = \mathbf{0}$, $\mathbf{S}_i^{\text{s}} = \mathbf{0}$, 以及 $\beta = 0$, $\bar{\mathbf{M}}_{\text{wk}} = \mathbf{0}$, $\bar{\mathbf{F}}_k^{\text{w}} = \mathbf{0}$, $\bar{\mathbf{T}}_k^{\text{w}} = \mathbf{0}$, $\bar{\mathbf{T}}_k^{\text{s}} = \mathbf{0}$, $\bar{\mathbf{S}}_k^{\text{w}} = \mathbf{0}$ 代入式 (24) 和式 (29), 可分别得到式 (40) 和式 (39). 因此, 流体-干基岩耦合情形同样是两种不同多孔介质耦合情形的特例.

综上所述, 流体、固体、饱和多孔介质之间的耦合均可统一在同一理论框架进行分析.

1.3 实施方法

以图 3(a) 所示的模型为例, 考虑海水-饱和海床-基岩水平成层体系在平面 P-SV 波垂直入射时的反应. 对于该问题, 可采用 Thomson-Haskell 传递矩阵方法 (transfer matrix method, TMM) 求得解析解^[31-33], 称为自由场, 做为有限元数值解的验证依据.

另外, 对于复杂地形, 或有散射体 (如海工结构) 存在的情形, 需要通过有限元数值方法进行求解.

因此,我们对图 3(a)所示的问题采用本文提出的有限元方法求解,计算模型如图 3(b)所示,在侧面和底面采用多次透射人工边界^[22],用于模拟无限域.在边界上采用传递矩阵方法得到的自由场作为波动输入.海水-饱和和海床-基岩体系中,内部点(除人工边界点和界面点外的其余节点)及界面点的响应计算,均采用统一的饱和多孔介质方程和不同饱和多孔介质间界面点的计算方法,即 2.1 节中的理论方法.具体实施时,在界面处设置一层“虚单元”,该单元的材料参数为零.这样,对于内部点的响应,按饱和多孔介质显式有限元方法计算;对于界面点的响应,没有界面连续条件约束的某些方向(对于文中所述情形,为 x 和 y 方向的液相等),其响应计算与内部点一样.对于有连续条件的方向,仅需每时步在节点对(如图 3(b)中 i 和 k 点)之间传递节点本构力和位移.基于此,编制了相应的三维有限元计算程序,以实现本文方法.

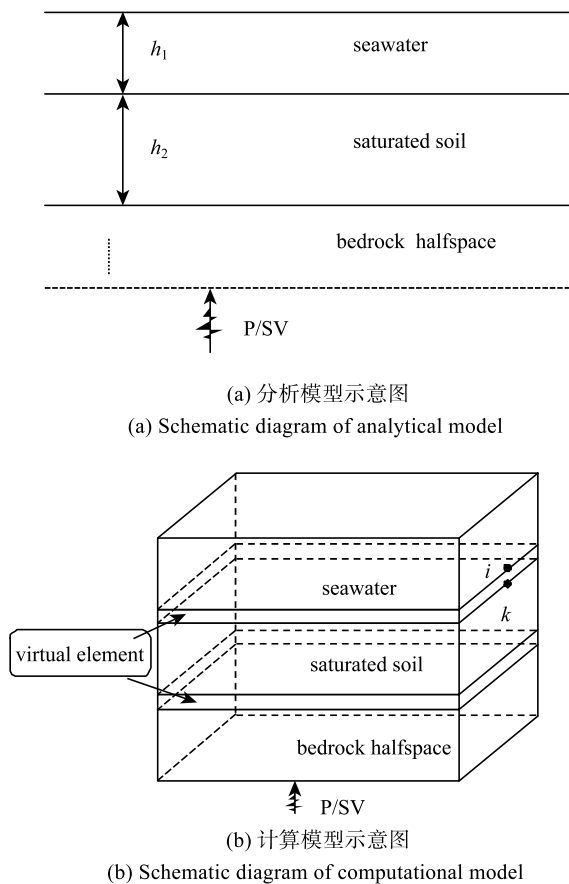


图 3 模型示意图和计算模型示意
Fig. 3 Schematic diagram of model

2 算例验证

采用如下线弹性本构

$$\sigma'_{ij} - (1 - \alpha)\delta_{ij}P = 2\mu e_{ij} + \delta_{ij}\lambda e \quad (41a)$$

$$P = -\alpha M e + M \zeta \quad (41b)$$

其中,根据文献[17-18], λ 和 μ 为固相骨架在排水情形时的拉梅常数, α 和 M 则为表征饱和多孔介质压缩性的常数,以压缩模量表示时为

$$\alpha = 1 - \frac{E_b}{E_u} \quad (42)$$

$$M = \frac{E_u^2}{E_u \left[n \left(\frac{E_u}{E_w} - 1 \right) + 1 \right] - E_b} \quad (43)$$

其中, E_u 和 E_b 分别为不排水和排水时饱和多孔介质的压缩模量, E_w 为孔隙流体的压缩模量, k_0 为渗透系数.

下面所有算例模型 x, y 方向尺寸为 $40 \text{ m} \times 40 \text{ m}$, 单元尺寸 $\Delta x = 1 \text{ m}$, 时间步距为 $\Delta t = 0.000 2 \text{ s}$, 输入图 4 所示的单位脉冲, $\Delta x \leq \lambda_{\min}/10$, 满足精度要求,其中 λ_{\min} 为所需模拟的最小波长.所有材料参数见表 1.

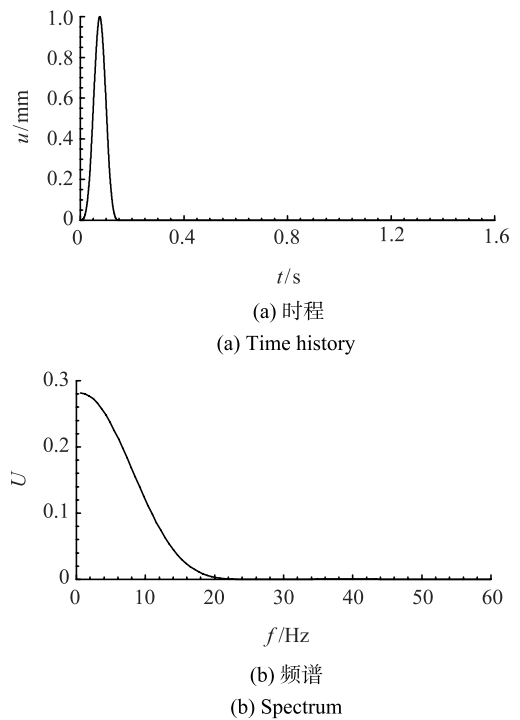


图 4 输入脉冲
Fig. 4 Input pulse

表1 材料参数表

Table 1 Parameters of material

Media	Prosimy β	μ_0	$\rho_s/(\text{kg}\cdot\text{m}^{-3})$	$\rho_w/(\text{kg}\cdot\text{m}^{-3})$	ν	G/MPa	E_w/GPa	M/GPa	α	$k_0/\mu\text{m}^2$
seawater	1	0	0	1000	0.49	0	2.25	2.25	1	1
saturated soil	0.26	0.001	2000	1000	0.49	83.2	2.25	4.78	0.697	10^{-7}
bedrock	0	0	2500	0	0.2	480	0	—	0	0

2.1 海水-干土情形

海水-干基岩模型如图 5 所示. 图 6 和图 7 分别为 P 波和 SV 波入射时的响应. 从图中可以看出, 传递矩阵方法得到的解析解 [33] 与有限元计算的数值解结果完全吻合. 对于 SV 波垂直入射情形, 由于没

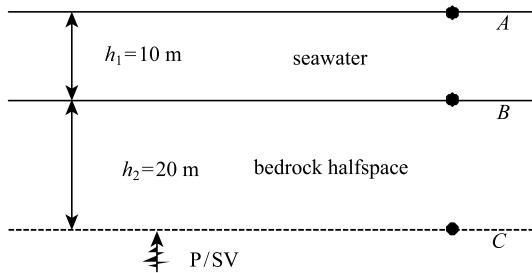
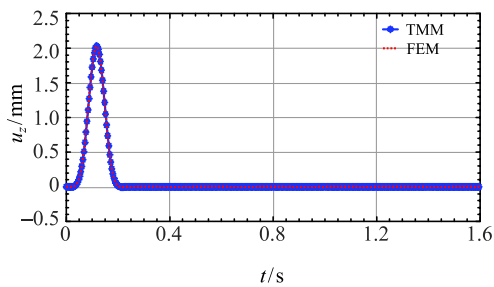
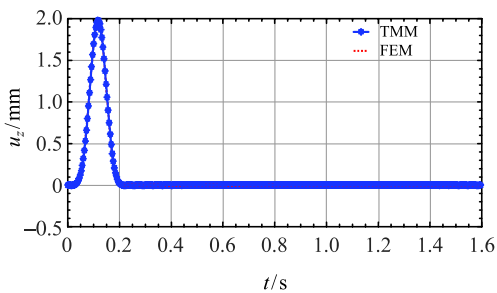


图 5 海水-基岩模型

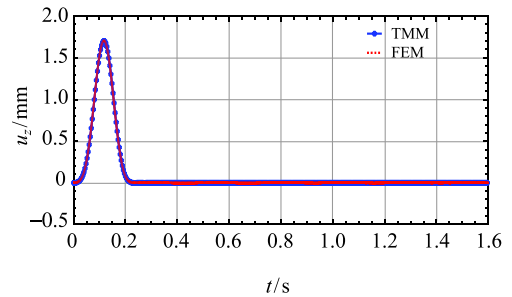
Fig. 5 Seawater-bedrock model



(a) A点海水位移
(a) Seawater displacement at point A

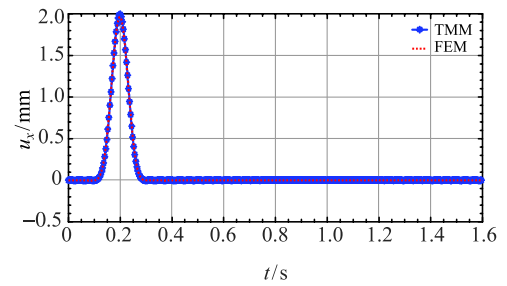


(b) B点海水位移
(b) Seawater displacement at point B

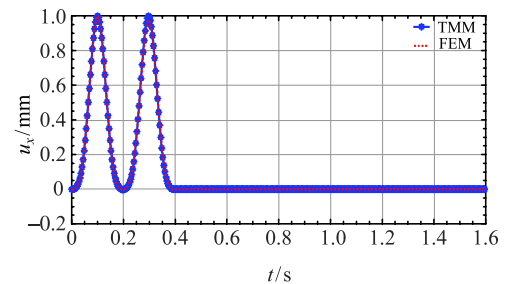


(c) C点基岩位移
(c) Bedrock displacement at point C

图 6 P 波入射时海水-基岩系统的位移响应
Fig. 6 Displacement of seawater-bedrock system for P wave incidence



(a) B点基岩位移
(a) Bedrock displacement at point B



(b) C点基岩位移
(b) Bedrock displacement at point C

图 7 SV 波入射时海水-基岩系统的位移响应
Fig. 7 Displacement of seawater-bedrock system for SV wave incidence

考虑流体黏性，流体中不能传播 SV 波，A 点没有响应，该情形与基岩半空间相同，图中结果也验证了这点.

2.2 海水-饱和土情形

将海床考虑为饱和土情形，海水-饱和海床模型如图 8 所示. 图 9 和图 10 分别为 P 波和 SV 波入射时的响应. 从图中可以看出，数值解与解析解完全重合.

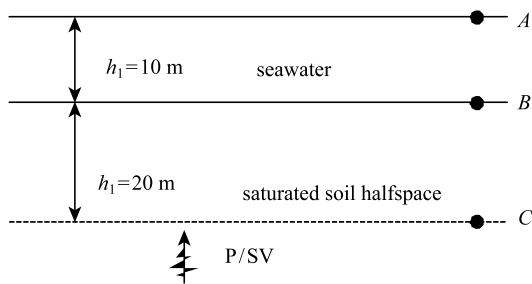
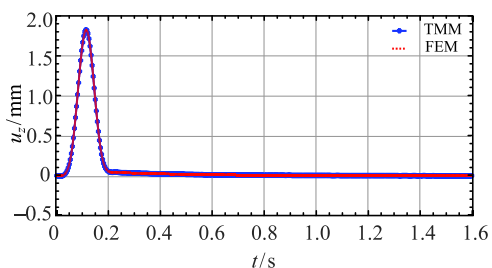


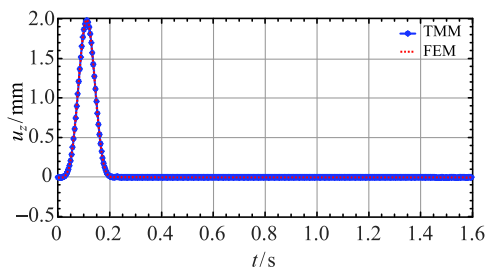
图 8 海水-饱和土模型

Fig. 8 Seawater-saturated soil model



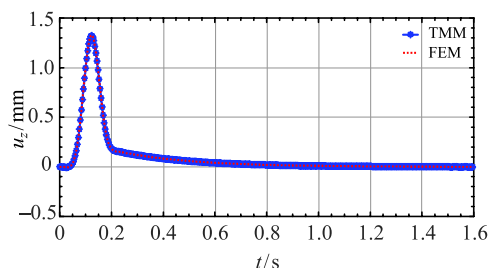
(a) A点海水位移

(a) Seawater displacement at point A



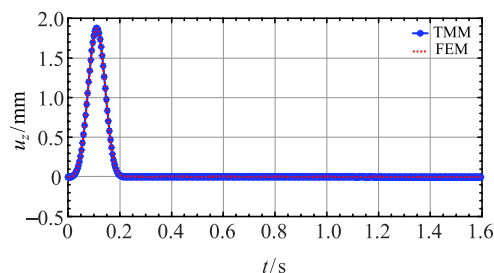
(b) B点饱和土固相位移

(b) Solid displacement at point B



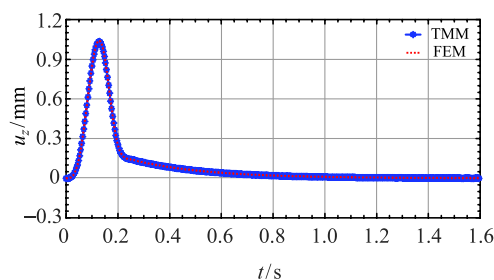
(c) B点饱和土液相位移

(c) Liquid displacement at point B



(d) C点饱和土固相位移

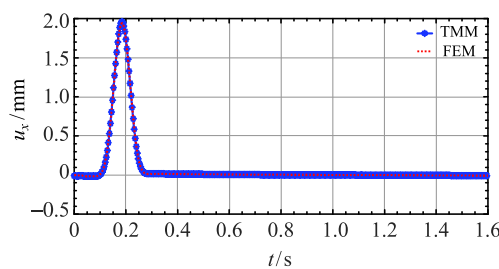
(d) Solid displacement at point C



(e) C点饱和土液相位移

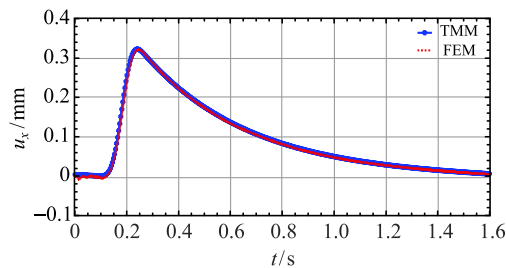
(e) Liquid displacement at point C

图 9 P 波入射时海水-饱和土系统的位移响应
Fig. 9 Displacement of seawater-saturated soil system for P wave incidence



(a) B点饱和土固相位移

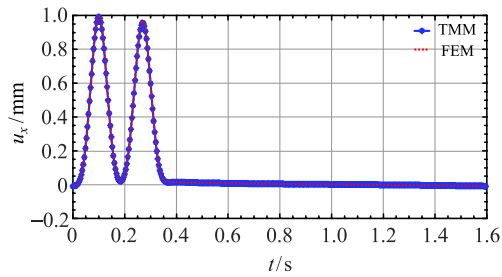
(a) Solid displacement at point B



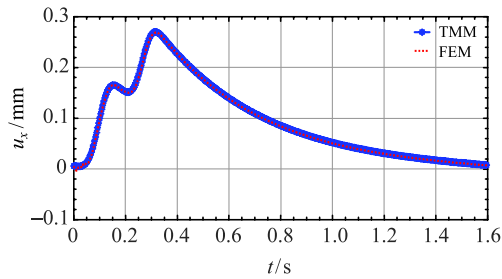
(b) B点饱和土液相位移

(b) Liquid displacement at point B

图 10 SV 波入射时海水-饱和土系统的位移响应
Fig. 10 Displacement of seawater-saturated soil system for SV wave incidence



(c) C点饱和土固相位移
(c) Solid displacement at point C



(d) C点饱和土液相位移
(d) Liquid displacement at point C

图 10 SV 波入射时海水-饱和土系统的位移响应(续)
Fig. 10 Displacement of seawater-saturated soil system for SV wave incidence(continued)

通过上述三个算例，验证了本文统一计算框架的有效性，以及并行计算的可行性。

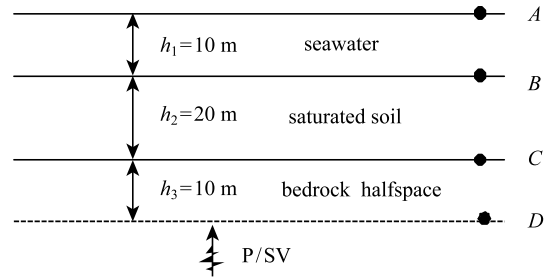
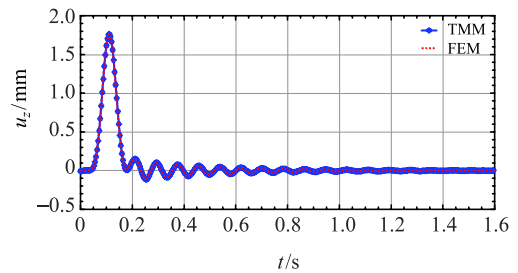
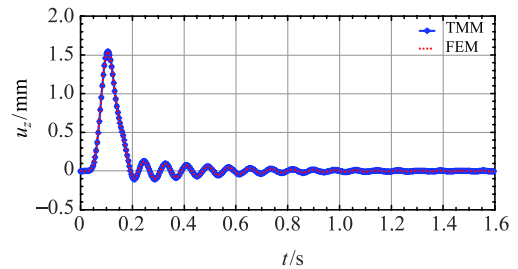


图 12 海水-饱和土-基岩模型

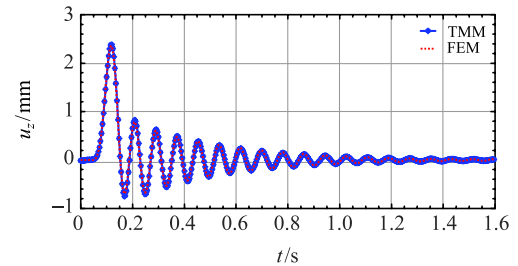
Fig. 12 Seawater-saturated soil-bedrock



(a) A点海水位移
(a) Seawater displacement at point A



(b) B点饱和土固相位移
(b) Solid displacement at point B



(c) B点饱和土液相位移
(c) Liquid displacement at point B

图 13 P 波入射时海水-饱和土-基岩体系的位移响应
Fig. 13 Displacement of seawater-saturated soil-bedrock system for P wave incidence

2.3 海水-饱和海床-基岩情形 (并行算例)

大规模计算通常采用并行技术以提高效率. 这里, 对于海水-饱和海床-基岩模型, 我们采用串行和并行(三进程, 如图 11 所示) 两种计算方法. 两进程的计算区域重叠一层单元(如图 11 中阴影部分), i 点为进程 1 的内部点, 为进程 2 的边界点, 因此在进程 1 中计算 i 点的响应, 通过 MPI 通讯协议传递给进程 2, 同样 j 点的响应在进程 2 计算, 然后传递给进程 1. 将计算结果与解析解进行对比, 见图 13 和图 14. 由图可知, 除了 SV 波垂直入射时, 饱和土液相位移略有误差外, 其余响应均与解析解重合. 串行和并行计算时间分别为 91 min 和 34 min, 并行计算时间大致为串行的 1/3, 大大提高了计算效率.

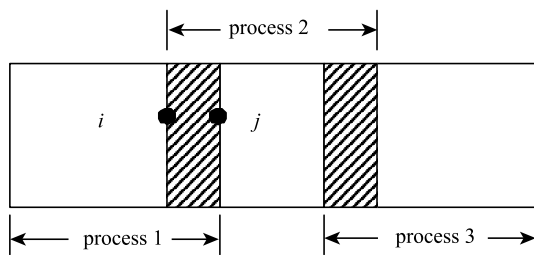
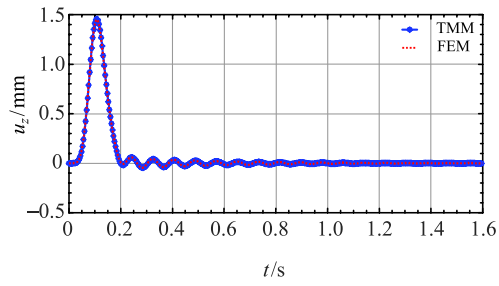
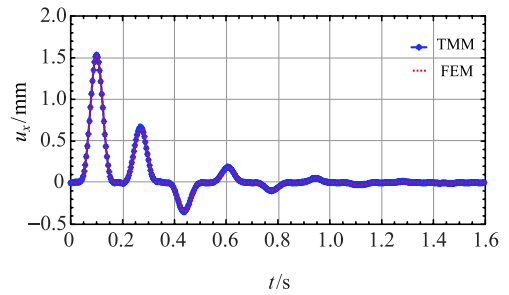


图 11 并行计算示意图

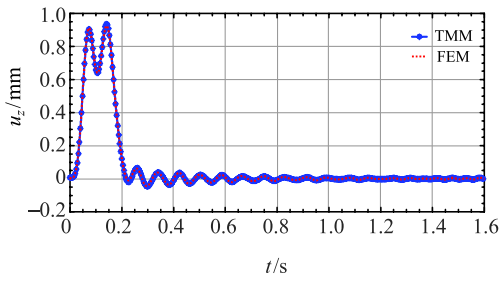
Fig. 11 Schematic diagram of parallel computation



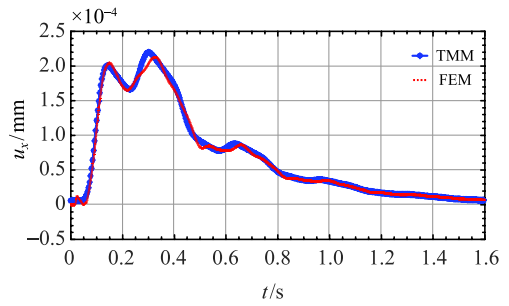
(d) C点基岩位移
(d) Bedrock displacement at point C



(c) C点饱和土固相位移
(c) Solid displacement at point C



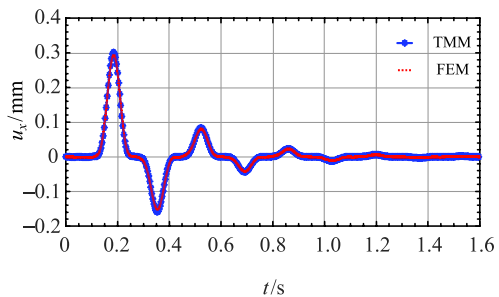
(e) D点基岩位移
(e) Bedrock displacement at point D



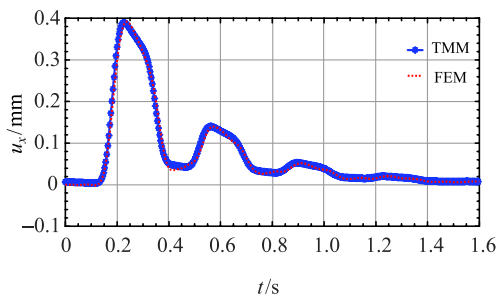
(d) C点饱和土液相位移
(d) Liquid displacement at point C

图 13 P 波入射时海水-饱和土-基岩体系的位移响应(续)

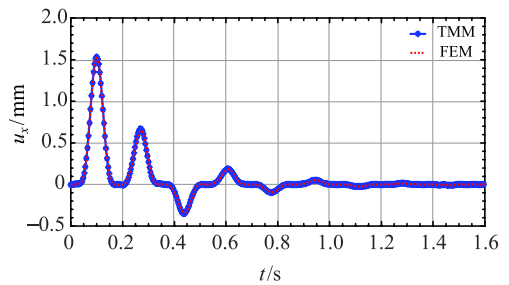
Fig. 13 Displacement of seawater-saturated soil-bedrock system for P wave incidence(continued)



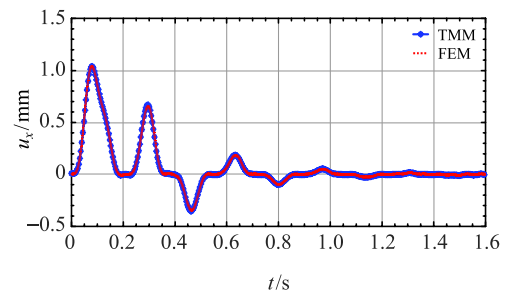
(a) B点饱和土固相位移
(a) Solid displacement at point B



(b) B点饱和土表面液相
(b) Liquid displacement at point B



(e) C点基岩位移
(e) Bedrock displacement at point C



(f) D点基岩位移
(f) Bedrock displacement at point D

图 14 SV 波入射时海水-饱和土-基岩体系的位移响应

Fig. 14 Displacement of seawater-saturated soil-bedrock system for SV wave incidence

3 结论

本文将理想流体、固体、饱和多孔介质之间的耦合分析纳入到统一计算框架,建立了集中质量显式有限元求解方法,并编制了相应的三维并行分析程序.分析了半无限海水-饱和海床、海水-弹性基岩、海水-饱和海床-弹性基岩三种情形在 P-SV 波垂直入射时的动力响应,通过与传递矩阵方法得到的结果进行对比,验证了该统一计算框架的有效性以及并行计算的可行性.

文中的算例采用线弹性本构,但公式推导只涉及本构力,可以适用于非线性情形.界面点的精度与内域点一致,取决于有限元空间离散精度和时步积分格式的精度,可以采用其他格式满足所需精度要求.文中算例未出现失稳现象,但耦合计算格式的稳定性需另做讨论.另外,本文只考虑了水平成层情形,通过考虑界面的方向导数,该方法可以推广到复杂海底地形情形,结合并行技术,可以模拟大规模海底地震动问题以及海水-海床-结构体系的地震响应问题,也可为海洋声学及海洋地震勘探提供正演分析方法.

参 考 文 献

- Nakamura T, Takenaka H, Okamoto T, et al. FDM Simulation of seismic-wave propagation for an aftershock of the 2009 Suruga Bay earthquake: Effects of ocean-bottom topography and seawater layer. *Bulletin of Seismological Society of America*, 2012, 102(6): 2420-2435
- Petukhin A, Iwata T, Kagawa T. Study on the effect of the oceanic water layer on strong ground motion simulations. *Earth Planets Space*, 2010, 62: 621-630
- Jianhong Y. Seismic response of poroelastic seabed and composite breakwater under strong earthquake loading. *Bulletin of Earthquake Engineering*, 2012, 10: 1609-1633
- Cheng XS, Xu WW, Yue CQ, et al. Seismic response of fluid-structure interaction of undersea tunnel during bidirection earthquake. *Ocean Engineering*, 2014, 75: 64-70
- Jin HL, Seo SI, Mun HS. Seismic behaviors of a floating submerged tunnel with a rectangular cross-section. *Ocean Engineering*, 2016, 127: 32-47
- Farhat C, Lesoinne M, LeTallec P. Load and motion transfer algorithms for fluid/structure interaction problems with non-matching discrete interfaces: Momentum and energy conservation, optimal discretization and application to aeroelasticity. *Computer Methods in Applied Mechanics & Engineering*, 1998, 157(1): 95-114
- Farhat C, Lesoinne M. Two efficient staggered algorithms for serial and parallel solution of three-dimensional nonlinear transient aeroelastic problems. *Computer Methods in Applied Mechanics & Engineering*, 2000, 182: 499-515
- Farhat C, Zee KGV, Geuzaine P. Provably second-order time-accurate loosely-coupled solution algorithms for transient nonlinear computational aeroelasticity. *Computer Methods in Applied Mechanics & Engineering*, 2006, 195(17): 1973-2001
- Bathe KJ, Zhang H. Finite element developments for general fluid flows with structural interactions. *International Journal for Numerical Methods in Engineering*, 2010, 60(1): 213-232
- Degroote J, Haelterman R, Annerel S, et al. Performance of partitioned procedures in fluid-structure interaction. *Computers & Structures*, 2010, 88(7): 446-457
- Hou G, Wang J, Layton A. Numerical methods for fluid-structure Interaction — A review. *Communications in Computational Physics*, 2012, 12(2): 337-377
- Habchi C, Russeil S, Bougeard D, et al. Partitioned solver for strongly coupled fluid-structure interaction. *Computers & Fluids*, 2013, 71(1): 306-319
- Mehl M, Uekermann B, Bijl H, et al. Parallel coupling numerics for partitioned fluid-structure interaction simulations. *Computers & Mathematics with Applications*, 2016, 71(4): 869-891
- Bungartz HJ, Lindner F, Gatzhammer B, et al. preCICE — A fully parallel library for multi-physics surface coupling. *Computers & Fluids*, 2016, 141: 250-258
- Banks JW, Henshaw WD, Kapila AK, et al. An added-mass partition algorithm for fluid-structure interactions of compressible fluids and nonlinear solids. *Journal of Computational Physics*, 2016, 305(C): 1037-1064
- Basting S, Quaini A, Glowinski R. Extended ALE Method for fluid-structure interaction problems with large structural displacements. *Journal of Computational Physics*, 2016, 331(C): 312-336
- Biot MA. Theory of propagation of elastic waves in a fluid-saturated porous solid. *Acoust Soc Am*, 1956, 28: 168-191
- Biot MA. Mechanics of deformation and acoustic propagation in porous media. *Journal of Applied Physics*, 1962, 33(4): 1482-1498
- Komatitsch D, Barnes C, Tromp J. Wave propagation near a fluid-solid interface: A spectral-element approach. *Geophysics*, 2000, 65(2): 623-631
- Link G, Kaltenbacher M, Breuer M, et al. A 2D finite-element scheme for fluid-solid-acoustic interactions and its application to human phonation. *Computer Methods in Applied Mechanics & Engineering*, 2009, 198(41): 3321-3334
- 李伟华. 考虑水-饱和土场地-结构耦合时的沉管隧道地震反应分析. 防灾减灾工程学报, 2010, 30(6): 607-613(Li Weihua. Seismic Response analysis of immersed tube tunnels considering water saturated soil site structure coupling. *Journal of Disaster Prevention and Mitigation Engineering*, 2010, 30(6): 607-613(in Chinese))
- 廖振鹏. 工程波动理论导论. 第 2 版. 北京: 科学出版社, 2002: 136-285 (Liao Zhenpeng. Introduction to Wave Motion Theories in Engineering(2nd edn). Beijing: Science Press, 2002: 136-285 (in Chinese))
- 邢浩洁, 李鸿晶. 透射边界条件在波动谱元模拟中的实现: 二维波动. 力学学报, 2017, 49(4): 894-906 (Xing Haojie, Li Hongjing. Implementation of multi-transmitting boundary condition for wave motion simulation by spectral element method: Two dimension case. *Chinese Journal of Theoretical and Applied Mechanics*, 2017, 49(4):

- 894-906 (in Chinese))
- 24 谷音, 刘晶波, 杜修力. 三维一致粘弹性人工边界及等效粘弹性边界单元. *工程力学*, 2007, 24(12): 31-37(Gu Lin, Liu Jingbo, Du Xuli. Three-dimensional uniform viscoelastic artificial boundary and equivalent viscoelastic boundary element. *Journal of Engineering Mechanics*, 2007, 24(12): 31-37(in Chinese))
- 25 刘晶波, 宝鑫, 谭辉等. 波动问题中流体介质的动力人工边界. *力学学报*, 2017, 49(6): 1418-1427 (Liu Jingbo, BaoXin, Tan Hui, et al. Dynamical artificial boundary for fluid medium in wave motion problems. *Chinese Journal of Theoretical and Applied Mechanics*, 2017, 49(6): 1418-1427 (in Chinese))
- 26 赵宇昕, 陈少林. 关于传递矩阵法分析饱和成层介质响应问题的讨论. *力学学报*, 2016, 48(5): 1145-1158 (Zhao Yuxin, Chen Shaolin. Discussion on the matrix propagator method to analyze the response of saturated layered media. *Chinese Journal of Theoretical and Applied Mechanics*, 2016, 48(5): 1145-1158 (in Chinese))
- 27 刘晶波, 谭辉, 宝鑫等. 土-结构动力相互作用分析中基于人工边界子结构的地震波动输入方法. *力学学报*, 2018, 50(1): 32-43 (Liu Jingbo, Tan Hui, Bao Xin, et al. The seismic wave input method for soil-structure dynamic interaction analysis based on the substructure of artificial boundaries. *Chinese Journal of Theoretical and Applied Mechanics*, 2018, 50(1): 32-43 (in Chinese))
- 28 陈少林, 廖振鹏, 陈进. 两相介质近场波动模拟的解耦方法. *地球物理学报*, 2005, 48(4): 909-917 (Chen Shaolin, Liao Zhenpeng, Chen Jin. Decoupling method for near-field wave simulation of two-phase media. *Journal of Geophysics*, 2005, 48(4): 909-917 (in Chinese))
- 29 Deresiewicz H, Rice JT. The effect of boundaries on wave propagation in a liquid-filled porous solid: V. Transmission across a plane interface. *Bull Seis Soc Am*, 1964, 54(1): 409-416
- 30 Deresiewicz H. The effect of boundaries on wave propagation in a liquid-filled porous solid: VII. Surface waves in a half-space in the presence of a liquid layer. *Bull Seis Soc Am*, 1964, 54(1): 425-430
- 31 Thomson WT. Transmission of elastic waves through a stratified solid media. *Journal of Applied Physics*, 1950, 21: 89-93
- 32 Haskell NA. The dispersion of surface waves on multilayered media. *Bull Seismol Soc Am*, 1953, 43: 17-34
- 33 柯小飞, 陈少林, 张洪翔. P-SV 波入射时海水-层状海床体系的自由场分析. *振动工程学报*, 2018, 录用 (Ke Xiaofei, Chen Shaolin, Zhang Hongxiang. Freefield analysis of seawater-layered seabed system at P-SV wave incident. *Journal of Vibration Engineering*, 2018, Accepted (in Chinese))